Table II. Best Fit of Energy Transitions and g and μ_{eff} Values

Energy of Transition, cm^{-1}			
calcd	obsd	calcd	obsd
5303		17 739	17 300
5417		17 797	
5658		18 161	
5736		18 232	
6425		21 405	
6471		21 417	21 400
7212	7100		
7366			
11 354			
11 504			
12 411			
12 506	12600		

g Values					
	calcd	obsd		calcd	obsd
g_1	2.04	2.05	g_3	4.84	4.7
g_2	3.86	4.0			

μ_{eff} Values, μ_B					
temp, K	obsd	calcd	temp, K	obsd	calcd
300	4.22	4.22	88	4.24	4.18

to the observed ones, with a sequence of excited levels in order of decreasing energy: A_2, E, E, A_2. Actually the order of the levels in the low-frequency region is not so well settled since many overlapping levels are present.

The usual variation of the e_π/e_σ ratio, although affecting to some extent the energy of the levels, does not greatly modify their order. It affects however to some extent the relative energies of the highest $^4A_2$ and ^4E levels, negative values tending to decrease the separation.

We wanted also to check what might be the effect on the energy levels of varying the N_{ax}-Co-N_{eq} angle in the range from 109.44°, the tetrahedral value, to 90°. The computed levels are shown in Figure 5. It is apparent that with this variation the $^4A_2(P)$-$^4E(P)$ separation tends to increase, as does also the energy of ^4E relative to the ground $^4A_2$ level. The levels in the low-frequency region follow a less definite pathway. In particular the energy relative to the ground state of the lowest $^4A_2$ levels is calculated to have a maximum at ~100°.

The best fit of the electronic transitions we were able to find is given in Table II together with the calculated g and μ values. The agreement is fully satisfactory for all the calculated properties. The values of the parameters used for the equatorial donors are much larger than usually found for pyrazole-type ligands.[16-21] As a matter of fact, the calculated Dq value ($Dq = 3e_\sigma - 4e_\pi$) for the equatorial ligand is 1500 cm^{-1}, much higher than 1000 cm^{-1} suggested by Jesson for poly(pyrazolyl)borates[12a] and also much higher than the value of 1100 cm^{-1} found by Reedijk[20] and 1200 cm^{-1} found by us for pyrazole.[17]

If we try to understand the large Dq value required for the equatorial donor atoms, a structural comparison may be required. As a matter of fact in the present case the metal to equatorial nitrogen distance is on the average 194 pm,[4] which is somewhat shorter than the average 197 pm seen in the poly(pyrazolyl)borate complexes[12b] and much shorter than the 200-215 pm seen in the octahedral pyrazole complexes.[22] Although it may be surprising that a variation of 3 pm determines such a large increase in the ligand field strength, we believe that this is the only rationale for justifying the unusal electronic spectra of $[Co(MeTPyEA)](BPh_4)_2$.

Registry No. $[Co(MeTPyEA)](BPh_4)_2$, 77417-18-6; $[Co(NCS)(MeTPyEA)]BPh_4$, 77417-20-0.

(16) Reedijk, J.; Harsen, J. C.; van Koningsveld, H.; van Kralingen, C. G. *Inorg. Chem.* **1978**, *17*, 1990.
(17) Bencini, A.; Benelli, C.; Gatteschi, D.; Zanchini, C. *Inorg. Chem.* **1980**, *19*, 1301.
(18) Roundhill, S. G. N.; Roundhill, D. M.; Bloomquist, D. R.; Landee, C.; Willett, R. D.; Dooley, D. M. Gray, H. B. *Inorg. Chem.* **1979**, *18*, 831.
(19) O'Young, C. L.; Devon, J. C.; Lilienthal, H. R.; Lippard, S. J. *J. Am. Chem. Soc.* **1978**, *100*, 7291.
(20) Vermaas A.; Groenevald, W. L.; Reedijk, J. *Z. Naturforsch., A* **1977**, *32A*, 632.
(21) Thompson, J. S.; Sorrell, T.; Marks, T. J.; Ibers, J. A. *J. Am. Chem. Soc.* **1979**, *101*, 4193.
(22) Reimann, C. W.; Mighell, A. D.; Maner, A. F. *Acta Crystallogr.* **1967**, *23*, 135.

Contribution from the Departments of Chemistry, Faculty of Science, Shinshu University, Asahi, Matsumoto 390, Japan, and Miami University, Oxford, Ohio 45056

^{19}F and ^{13}C NMR Study of the Kinetics of Ligand-Exchange Reactions in Oxovanadium(IV) Complexes

OSAMU YOKOYAMA, HIROSHI TOMIYASU, and GILBERT GORDON*

Received January 6, 1981

The kinetics of fluoride ion exchange in the oxovanadium(IV) glycine and fluoride mixed complex, VO(gly)glyF$^-$, and oxalate exchange in (dioxalato)oxovanadium(IV), $VO(ox)_2^{2-}$, have been studied by means of ^{19}F NMR and ^{13}C NMR methods. The equilibrium and formation reactions of these complexes have also been studied by using spectrophotometric and stopped-flow measurements. In every case, the reactions were found to be first order in both the entering ligand and the VO^{2+} complex. The overall rate is determined primarily by the charge on the ligand and on the complex, and the chelation process is not dissociation controlled. The activation parameters obtained are as follows: for F$^-$ exchange on VO(gly)glyF$^-$, $\Delta H^\ddagger = 33.2 \pm 1.6$ kJ mol^{-1} and $\Delta S^\ddagger = -51.7 \pm 5.3$ J K^{-1} mol^{-1}; for oxalate exchange on $VO(ox)_2^{2-}$, $\Delta H^\ddagger = 39.8 \pm 1.9$ kJ mol^{-1} and $\Delta S^\ddagger = -51.6 \pm 5.8$ J K^{-1} mol^{-1} at pH 6.50 and $\Delta H^\ddagger = 51.0 \pm 2.6$ kJ mol^{-1} and $\Delta S^\ddagger = -7.6 \pm 8$ J K^{-1} mol^{-1} at pH 2.89.

During the past decade the kinetics of ligand substitution reactions for oxovanadium(IV) complexes have been of particular interest.[1-12] The ^{17}O NMR studies[1-3] were important in the early studies, which were concerned with the water-exchange reaction for $VO(H_2O)_5^{2+}$ and other related com-

* To whom correspondence should be addressed at Miami University.

(1) Reuben, J.; Fiat, D. *Inorg. Chem.* **1967**, *6*, 579.
(2) Wuthrich, K.; Connick, R. E. *Inorg. Chem.* **1967**, *6*, 583.
(3) Wuthrich, K.; Connick, R. E. *Inorg. Chem.* **1968**, *7*, 1377.
(4) Tomiyasu, H.; Dryer, K.; Gordon, G. *Inorg. Chem.* **1972**, *11*, 2409.
(5) Tomiyasu, H.; Ito, S.; Tagami, S. *Bull. Chem. Soc. Jpn.* **1974**, *47*, 2843.
(6) Tomiyasu, H.; Gordon, G. *Inorg. Chem.* **1976**, *15*, 870.
(7) Nishizawa, M.; Saito, K. *Inorg. Chem.* **1978**, *17*, 3676.
(8) Nishizawa, M.; Saito, K. *Bull. Chem. Soc. Jpn.* **1978**, *51*, 483.
(9) Angerman, N. S.; Jordan, R. E. *Inorg. Chem.* **1969**, *8*, 65.

0020-1669/82/1321-1136$01.25/0

plexes.

It was found that water molecules in the equatorial and the axial positions behave completely differently.[4] The rate and mechanism for the replacement of coordinated water in the equatorial positions by various ligands were later studied by stopped-flow and temperature-jump relaxation methods.[5-7,11]

The kinetic behavior of bidentate[5,6] and multidentate ligands[8,9] has been reported, but the role of axial vs. equatorial monodentate intermediates and competition between substitution by solvent and/or anions and ring closure are not very well understood.[6]

In this paper we report the kinetics of reactions 1–5 using

$$VO(gly)_2 + F^- \rightleftharpoons VO(gly)glyF^- \quad (1)$$

$$VO(gly)glyF^- + {}^*F^- \rightleftharpoons VO(gly)gly{}^*F^- + F^- \quad (2)$$

$$VO(ox)_2^{2-} + {}^*ox^{2-} \rightleftharpoons VO(ox)({}^*ox)^{2-} + ox^{2-} \quad (3)$$

$$VO(ox)_2^{2-} + {}^*Hox^- \rightleftharpoons VO(ox)({}^*ox)^{2-} + Hox^- \quad (4)$$

$$VO(H_2O)_5^{2+} + 2H_2ox \rightarrow VO(ox)_2^{2-} + 4H^+ \quad (5)$$

^{19}F NMR and ^{13}C NMR spectrometry as well as the stopped-flow techniques in an attempt to better understand the role of intermediates in oxovanadium(IV) substitution reactions (for the purpose of convenience, glycine and oxalate will be abbreviated gly (or Hgly) and ox (or Hox), respectively, and water in the axial position will not be shown except for $VO(H_2O)_5^{2+}$).

Experimental Section

The preparation and methods of chemical analysis used for the oxovanadium(IV) solutions have been described in previous papers.[4,6] The methods used to purify sodium hydroxide and glycine have also been described previously.[4] Reagent grade sodium fluoride, sodium oxalate, and potassium oxalate were used directly without further purification. The pH of the solution was measured with a Hitachi-Horiba Model F-7s pH meter. The spectrophotometric measurements were made at 25 °C on a Shimadzu MPS-50L spectrometer.

Stopped-flow measurements were made at 14 °C and at 740 nm by an instrument manufactured by the Union Scientific Engineering Co., Ltd. A JEOL JNM-MH-100 NMR spectrometer equipped with a JEOL JNM-VT-3B temperature controller and a JNM-FX-90Q spectrophotometer were used for the NMR measurements. Temperatures were calibrated[6] by the chemical shift difference between the methyl and the hydroxyl proton signals of methanol. At least 2000 individual signals were integrated for all of the ^{13}C NMR measurements.

The relaxation time, T_2, of ^{13}C NMR signals is usually very long in pure solvents, and the values of T_2 are difficult to obtain from conventional line-width measurements. For the pulsed NMR technique used here, accurate values for long T_2 relaxation times were obtained by means of the Carr–Purcell–Meiboom–Gill method.[16] However, in the presence of paramagnetic species such as VO^{2+} the values of T_2 were considerably smaller (0.1 s). Under these conditions, pulse intervals in the range of approximately 2 s were used and several thousand spectra were readily integrated in relatively short time periods (2–3 h) without any apparent decomposition. The corresponding ^{13}C relaxation times were calculated directly from the NMR measurements by using the techniques reported in detail elsewhere.[4-6,16]

Results and Discussion

Equilibrium between $VO(gly)_2$ and Fluoride Ion. When 10^{-2} M F^- is added to solutions of (diglycinato)oxovanadium(IV), $VO(gly)_2$, the absorption spectrum changes as is shown by Figure 1. Although it was anticipated from earlier studies[13]

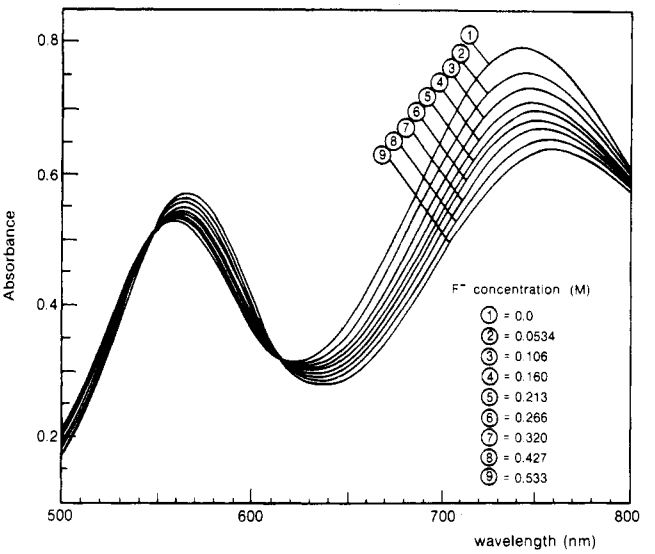

Figure 1. Absorption spectra for the $VO(gly)_2F^-$ species at various F^- concentrations with 0.0166 M $[VO^{2+}]_t$ and 1.64 M glycine at pH 7.07 and 1.0 M $NaClO_4$.

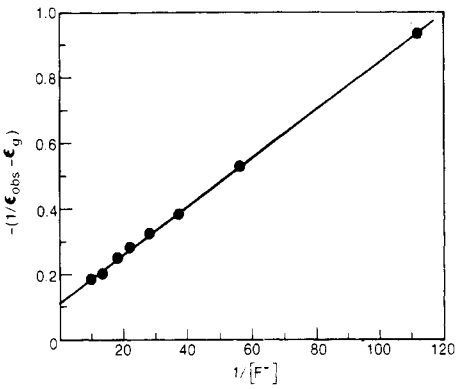

Figure 2. Plot of apparent molar absorptivity as a function of reciprocal fluoride ion concentration with 0.0166 M $VO(gly)_2$ and 1.0 M $NaClO_4$.

that $VO(gly)_2$ interacts with F^- ion, the existence of isosbestic points at 540 and 610 nm indicates that only one species is formed from the addition of F^- ion to a $VO(gly)_2$ solution. The most probable reaction taking place upon the addition of F^- ion is

$$VO(gly)_2 + F^- \rightleftharpoons VO(gly)glyF^-$$

The stability constant for this process, K_1, can be obtained from eq 6, which is derived from Beer's law and eq 1. Here, ϵ_{obsd}

$$1/(\epsilon_{obsd} - \epsilon_g) = 1/(\epsilon_f - \epsilon_g) + [1/K_1(\epsilon_f - \epsilon_g)](1/[F^-]) \quad (6)$$

is the observed molar absorptivity for the VO^{2+} species, and ϵ_g and ϵ_f are those of $VO(gly)_2$ and $VO(gly)glyF^-$, respectively. It can be seen that the plot should be linear if $(\epsilon_{obsd} - \epsilon_g)^{-1}$ is plotted vs. $1/[F^-]$. Indeed, Figure 2 shows this linear relationship, which supports the validity of the reaction shown by means of eq 1. From the slope and intercept, values of $K_1 = 17.0 \pm 1.0\ M^{-1}$ and $\epsilon_f = 15.8 \pm 0.5\ M^{-1}\ cm^{-1}$ are calculated from the results at 740 nm.

The structure of this mixed-ligand complex, $VO(gly)glyF^-$, can be written as either I or II. Although the structure of

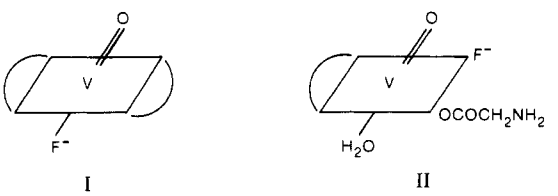

I II

(10) Jordan, R. B.; Angerman, N. S. *J. Chem. Phys.* **1968**, *48*, 3983.
(11) Kustin, K.; Pizer, R. *Inorg. Chem.* **1970**, *9*, 1536.
(12) Johnson, C. R.; Shepherd, R. E. *Bioinorg. Chem.* **1978**, *1*, 1.
(13) Tomiyasu, H.; Gordon, G. *J. Coord. Chem.* **1973**, *3*, 47.
(14) Ito, S.; Tomiyasu, H.; Ohtaki, H. *Bull. Chem. Soc. Jpn.* **1973**, *46*, 224.
(15) Swift, T. J.; Connick, R. E. *J. Chem. Phys.* **1962**, *37*, 307.
(16) Farrar, T. C.; Becker, E. D. "Pulse and Fourier Transform NMR"; Academic Press: New York, 1971.

Table I. Experimental and Calculated Absorbances at 750 nm for Solutions Containing VO^{2+}, $VOHox^{+}$, VO(ox), and $VO(ox)_2^{2-}$ as a Function of pH and H_2ox

$10^2[VO^{2+}]_t$,[a] M	$10^3[H_2ox]_t$,[a] M	pH	abs obsd	abs calcd
1.72	0.802	1.54	0.679	0.694
	1.60	1.09	0.602	0.610
	1.60	1.52	0.605	0.615
	3.21	1.52	0.623	0.638
	6.42	1.07	0.626	0.637
	6.42	1.53	0.665	0.679
	8.02	1.07	0.632	0.639
	16.03	1.54	0.761	0.752
	24.05	1.55	0.819	0.807
	32.06	1.56	0.855	0.837
1.62	6.20	1.79	0.621	0.644
	9.31	2.02	0.674	0.674
	10.86	2.02	0.691	0.687
	12.41	2.02	0.711	0.698
	13.96	2.02	0.726	0.714
	15.51	2.00	0.726	0.714
	17.06	2.00	0.737	0.719

[a] The quantity in the brackets represents total analytical concentrations.

this complex may not be determined directly by spectroscopy, structure II seems to be more reasonable considering the spectra of other related VO^{2+} glycine complexes.[12,13]

Equilibrium between VO^{2+} and Oxalate. The absorption spectra of VO^{2+} in the presence of oxalic acid differs from that of tetraaquooxovanadium(IV) ion, $VO^{2+}(aq)$. It was found that the absorbance at about 750 nm increases with increasing oxalic acid concentration. However, no additional changes in the spectra were observed if the concentration of oxalic acid was greater than 0.1 M at pH 1.6. These results suggest that complex formation between VO^{2+} and oxalic ion occurs, and from inferences in an earlier study,[13] the final product is most probably $VO(ox)_2^{2-}$.

Under the conditions when the oxalic acid concentration is less than 0.01 M at pH values below 1.5, the spectra are very similar to those reported for $VOHgly^{2+}$ [13] and $VOHmal^{+}$,[14] where glycine and bimalonate coordinate as unidentate ligands. In view of the similarity of the spectra, it would appear that the $VOHox^{+}$ complex, where Hox^{-} coordinates as a unidentate ligand, is formed in oxalic acid solutions under the conditions described here. At higher oxalate acid concentrations or at higher pH values, the monodentate oxalate coomplex, VO(ox), also appears to form and must be taken into account.

The stability constants for $VOHox^{+}$, VO(ox), and $VO(ox)_2^{2-}$ can be evaluated from the spectra at various pH values by the method described previously.[13] In Table I, the observed absorbances for VO^{2+} in the presence of oxalic acid are shown along with the calculated absorbance values obtained by using a least-squares analysis. The resulting values are $K_{1(Hox^-)} = 10.1\ M^{-1}$, $\beta_1 = 1.6 \times 10^5\ M^{-1}$, and $\beta_2 = 8.2 \times 10^9\ M^{-2}$, with the agreement between the observed and calculated spectra being better than ±2%.

^{19}F NMR for Exchange in VO(gly)glyF$^-$. The ^{19}F NMR spectrum of fluoride ion in aqueous solution at pH <7 shows line broadening as a result of the dissociation process appropriate to the reaction

$$HF + {}^*F^- \rightleftharpoons H{}^*F + F^-$$

However, at pH >7 the F^- exchange with HF can be neglected, and the ^{19}F NMR spectrum shows a very sharp line. Under these conditions above pH 7, line broadening is observed in the presence of the $VO(gly)glyF^-$ complex. This is consistent with the F^--exchange reaction

$$VO(gly)glyF^- + {}^*F^- \rightleftharpoons VO(gly)gly{}^*F^- + F^- \quad (2)$$

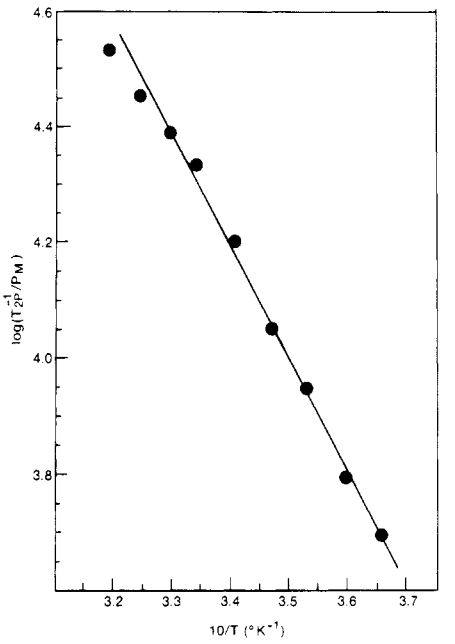

Figure 3. Plot of ^{19}F line width as a function of reciprocal temperature at pH 7.21 and 1.0 M $NaClO_4$, with $[VO^{2+}]_t = 2.12 \times 10^{-3}$ M, $[F^-]_t = 0.261$ M, and $[VO(gly)glyF^-] = 1.73 \times 10^{-3}$ M.

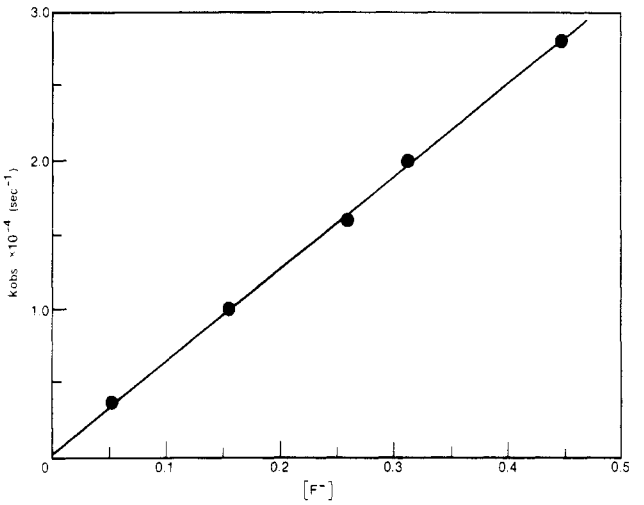

Figure 4. Plot of k_{obsd} as a function of fluoride ion concentration with 2.2×10^{-3} M $[VO^{2+}]_t$ at pH 7.2.

The line width becomes broader as the temperature increases, which is as anticipated for a chemically controlled exchange reaction. In Figure 3, log $[(1/T_{2p})/P_m]$ is plotted against the reciprocal temperature. The quantity T_{2p} is defined by[4,15]

$$1/T_{2p} = 1/T_2 - 1/T_{2a} = P_m/\tau_m \quad (7)$$

where T_2 is the relaxation time observed in the presence of VO^{2+} ion and T_{2a} is that in the absence of VO^{2+} and where P_m is that in the presence of VO^{2+}. In dilute solution, P_m can be approximated by

$$P_m = n[\text{complex}]/[\text{total ligands}]$$

where n is the number of coordinated ligands. The lifetime of a ligand in the environment of the coordination sphere, τ_m, is related to the first-order rate constant, k, as follows:

$$k = \tau_m^{-1} \quad (8)$$

It can be seen that Figure 3 is linear with negative slope. Clearly, the relaxation process is controlled by the chemical exchange process shown by reaction 2. The activation pa-

Table II. Rate Constants and Activation Parameters for Various Ligand-Substitution Reactions of VO^{2+} Complexes

reaction	rate const, M^{-1} s^{-1}	method	$\Delta H^{\ddagger}$, kJ mol^{-1}	$\Delta S^{\ddagger}$, J K^{-1} mol^{-1}
F^- exchange on VO(gly)glyF$^-$	$(6.4 \pm 0.3) \times 10^4$ (25 °C)	^{19}F NMR	$33._2 \pm 1._6$	$-51._7 \pm 5._3$
Hox$^-$ exchange[a] on $VO(ox)_2^{2-}$	$(6.6 \pm 0.6) \times 10^3$ (50 °C)	^{13}C NMR	$51._0 \pm 2._6$	$-7._6 \pm 8._6$
ox^{2-} exchange[b] on $VO(ox)_2^{2-}$	$(2.5 \pm 0.3) \times 10^3$ (50 °C)	^{13}C NMR	$39._8 \pm 1._9$	$-51._6 \pm 5._8$
formation of VO(gly)glyF$^-$ ($VO(gly)_2 + F^-$)	5.6×10^2 (15 °C)	stopped flow		
formation of $VO(ox)_2^{2-}$ ($VO^{2+} + Hox^-$)	$(7.0 \pm 1.3) \times 10^2$ (15 °C)	stopped flow		
formation of $VO(ox)_2^{2-}$ ($VO^{2+} + ox^{2-}$)	$(1.3 \pm 0.06) \times 10^4$ (15 °C)	stopped flow		

[a] pH 2.89. [b] pH 6.50.

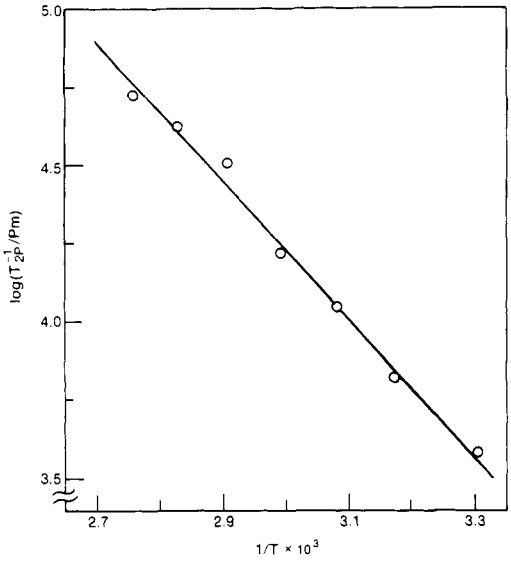

Figure 5. ^{19}F NMR as a function of reciprocal temperature with 0.012 M $[VO^{2+}]_t$ at pH 6.50.

rameters corresponding to reaction 2 are $\Delta H^{\ddagger} = 33._2 \pm 1._6$ kJ mol^{-1} and $\Delta S^{\ddagger} = -51._7 \pm 5._3$ J K^{-1} mol^{-1}. In Figure 4, the observed first-order rate constants are plotted as a function of fluoride ion concentration, demonstrating that the exchange reaction is first order in fluoride ion. Thus, k_{obsd} can be expressed as

$$k_{obsd} = k_{exptl}[F^-] \quad (9)$$

At pH 7.2, 1.0 M ionic strength, and 25 °C, the second-order rate constant, k_{exptl}, is $6.4 \pm 0.3 \times 10^4$ M^{-1} s^{-1}. These results are summarized in Table II.

^{13}C NMR of the Oxalate Exchange on $VO(ox)_2^{2-}$. The rate of oxalate exchange on $VO(ox)_2^{2-}$ was studied by means of ^{13}C nuclear magnetic resonance studies. The reaction can be expressed by eq 3 or 4. The rate of such an oxalate-exchange process might possibly be determined by using ^{17}O NMR spectrometry. However, the ^{17}O NMR spectrum of oxalate ion is not symmetrical because of the interference of the much larger concentration of the bulk $H_2{}^{17}O$ signal. The ^{13}C NMR spectrum of oxalate, on the other hand, shows only one singlet due to the $^{13}COO^-$ group. This makes the line-broadening information considerably easier to analyze with ^{13}C NMR than with ^{17}O NMR spectrometry.

The treatment of data is essentially the same as that described in the ^{19}F NMR experiments since the relaxation process is also controlled by chemical exchange as is noted in Figure 5, where log (T_{2p}^{-1}/P_m) is plotted against the reciprocal of the temperature at pH 6.50. Similar results are obtained at pH 2.89. The exchange rate can be obtained directly by using eq 7 and 8. The activation parameters obtained from the results of pH 6.50 (Figure 5) and pH 2.89 are summarized in Table II.

Table III. Observed Rate Constants for the Oxalate Exchange on $VO(ox)_2^{2-}$ as a Function of $[H_2ox]_t$ at 50 °C

$10^2[VO^{2+}]_t$, M	$[H_2ox]_t$, M	pH	$10^{-3}k_{obsd}$, s^{-1}
1.42	0.512	6.46	0.856 ± 0.040
1.52	0.686	6.36	1.50 ± 0.08
1.50	0.856	6.54	1.98 ± 0.06
1.49	1.018	6.73	2.05 ± 0.05
1.46	1.205	6.42	2.74 ± 0.04

Table IV. Observed Rate Constants for the Oxalate Exchange on $VO(ox)_2^{2-}$ as a Function of pH at 50 °C

$10^2[VO^{2+}]_t$, M	$[H_2ox]_t$, M	pH	$[ox^{2-}]$,[a] M	[Hox$^-$],[a] M	$10^{-3}k_{obsd}$, s^{-1}
1.50	0.433	2.14	0.011	0.385	2.64
1.50	0.531	3.73	0.280	0.250	2.10
1.50	0.533	4.11	0.389	0.144	2.03
1.50	0.525	4.50	0.456	0.069	1.58
1.67	0.585	5.10	0.563	0.022	1.51

[a] The concentrations of ox^{2-} and Hox$^-$ were calculated by using the values $pK_1 = 3.68$ and $pK_2 = 1.12$ obtained from: Sillen, L. G.; Martell, A. E. "Stability Constants"; The Chemical Society: London, 1971.

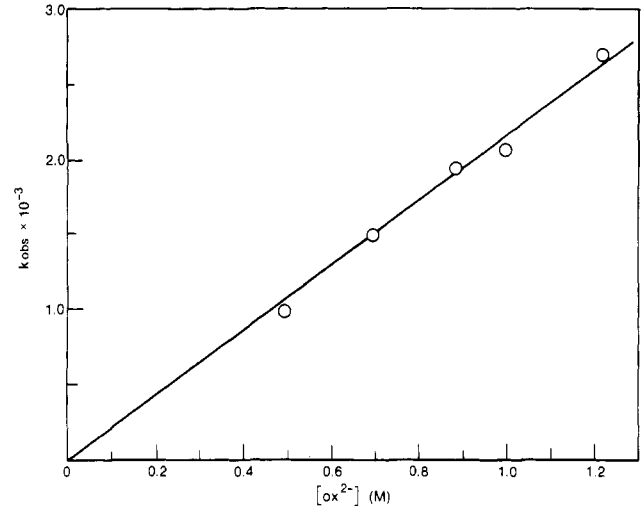

Figure 6. Graph of k_{obsd} as a function of oxalate ion concentration with 0.0102 M $[VO^{2+}]_t$ at pH 6.5 and 50 °C.

The observed rate constants for various concentrations of oxalic acid at about pH 6.5 are listed in Table III. Since oxalic acid exists mainly as the oxalate ion (ox^{2-}) (99.8%) in this pH region, the observed rate constant, k_{obsd}, was plotted against the $[ox^{2-}]$ concentration as is noted in Figure 6. As can be seen from these results, the exchange reaction is first order in $[ox^{2-}]$. Hence, the second-order rate constant, $k_{exptl,ox} = k_{obsd}/[ox^{2-}]$, was determined to be $(2.5 \pm 0.3) \times 10^3$ M^{-1} s^{-1}. The data at lower pH values are shown in Table IV. The exchange process was found to increase as the pH decreases below 6.5. This suggests that the species [Hox$^-$] could ac-

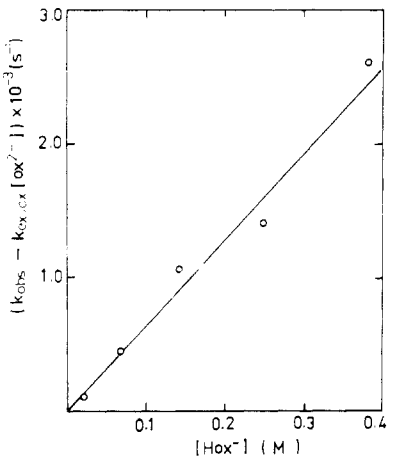

Figure 7. Plot of $\{k_{obsd} - k_{exptl,ox}[ox^{2-}]\}$ as a function of $[Hox^-]$ at 50 °C with 0.0102 M $[VO^{2+}]_t$.

celerate the exchange rate in the lower pH region. On the basis of this assumption, the following two exchange processes can be formulated:

$$VO(ox)_2^{2-} + {}^*ox^{2-} \rightleftharpoons VO(ox)({}^*ox)^{2-} + ox^{2-} \quad (3)$$

$$VO(ox)_2^{2-} + {}^*Hox^- \rightleftharpoons VO(ox)({}^*ox)^{2-} + Hox^- \quad (4)$$

Thus, the rate law based on these equations is expressed as

$$k_{obsd} = k_{exptl,Hox}[Hox^-] + k_{exptl,ox}[ox^{2-}] \quad (10)$$

or

$$k_{obsd} - k_{exptl,ox}[ox^{2-}] = k_{exptl,Hox}[Hox^-] \quad (10a)$$

Since the value of $k_{obsd} - k_{exptl,ox}$ was determined to be 2.5×10^3 M^{-1} s^{-1} at pH 6.5, the quantity $k_{obsd} - k_{exptl,ox}[ox^{2-}]$ can be plotted as a function of $[Hox^-]$ as is shown in Figure 7. If the mechanism shown by eq 3 and 4 is correct, the resulting plot as described by eq 10 and 10a should be linear with a zero intercept within the error limits set by the individual data points. As can be seen from Figure 7, the data are linear and the value of $k_{exptl,Hox}$ is determined to be $(6.6 \pm 0.6) \times 10^3$ M^{-1} s^{-1} at 50 °C.

Formation of VO(gly)glyF⁻ from VO(gly)$_2$. The formation of VO(gly)glyF⁻ from $VO(gly)_2$ was measured by the stopped-flow method. The reaction is expressed by eq 1. Since the concentration of fluoride ion was kept more than 10 times in excess of the VO^{2+} concentration, the reaction can be considered to be pseudo first order in $VO(gly)_2$. The stopped-flow data were fitted in terms of a first-order process. The observed second-order rate constant for the forward process (k_1) was determined to be 560 M^{-1} s^{-1} at 14 °C.

Needless to say, this value of the rate constant for reaction 1 supports structure II for the VO(gly)glyF⁻ complex since the rate of water exchange in the axial positions of VO^{2+} has been shown[2,3] to be extremely fast ($\sim 10^7$ s^{-1}). Clearly, the value of 560 M^{-1} s^{-1} would be too small, if an axial water molecule were assumed to be replaced by F^- ion in order to form structure I. On the other hand, the observed value of k_1 appears to be quite reasonable, if the NH_2 group of the coordinated glycine is replaced by fluoride ion, since the exchange rate between glycine and $VO(gly)_2$ as shown by eq 11

$$VO(gly)_2 + {}^*Hgly \rightleftharpoons VO(gly)({}^*gly) + Hgly \quad (11)$$

is reported[6] to be about 5×10^2 s^{-1}. Furthermore, the rate constant, $>k_1$ for the reverse of reaction 1, can be calculated from the relationship

$$k_1/k_{-1} = K_1 = 17.0 \text{ } M^{-1}$$

The calculated value of k_{-1} is 33 s^{-1} at 14 °C. The k_{-1} path

Table V. Rate Constants for the Formation[a] of $VO(ox)_2^{2-}$ as a Function of pH at 15 °C

pH	$10^2[Hox^-]$, M	$10^3[ox^{2-}]$, M	$10^{-2}k_s$, s^{-1}
3.82	5.68	23.14	2.99
3.49	6.69	12.85	2.12
3.44	6.81	11.60	1.85
3.34	7.01	9.45	1.69
3.09	7.33	5.56	1.35
2.93[b]	7.47	3.92	1.32
2.53[b]	7.52	1.57	0.829

[a] $[VO^{2+}]_t = 0.0221$ M and $[H_2ox]_t = 0.0789$ M. [b] Last two data were not included for least-squares calculation because of the low $[ox^{2-}]/[Hox^-]$ ratio.

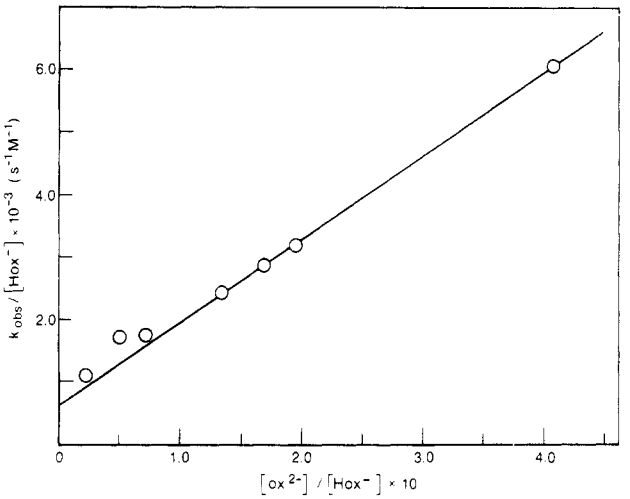

Figure 8. Typical rate constants as a function of the $[ox^{2-}]/[Hox^-]$ ratio at 25 °C, 0.0221 M $[VO^{2+}]_t$, and 0.0789 M $[H_2ox]_t$.

corresponding to the glycine chelation process[6] from the monodentate species is shown in eq 1a. It is interesting to

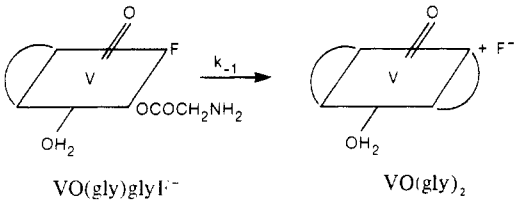

VO(gly)glyF⁻ $VO(gly)_2$ (1a)

note that the k_{-1} value is very similar to the rate constant (k_{11} = 35 s^{-1} at 25 °C) for the glycine solution process reported previously[6] (eq 12). The similarity in the rate constants for

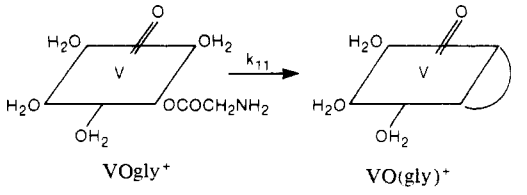

$VOgly^+$ $VO(gly)^+$ (12)

processes 1a and 12 suggests that the reactions are primarily controlled by association (i.e., chelation) of the glycine rather than by dissociation of the ligand being replaced (i.e., fluoride ion or a water molecule). Thus, the *chelation process is not dissociation controlled.*

Formation of $VO(ox)_2^{2-}$ from $VO(H_2O)_5^{2+}$. The rate of formation of $VO(ox)_2^{2-}$ from $VO(H_2O)_2^{2+}$ was also measured by using the stopped-flow method. The reaction is described by eq 5a, a modification of eq 5. Measurements were made

$$VO^{2+}(aq) + 2Hox^- \text{ (or } ox^{2-}) \rightarrow VO(ox)_2^{2-} + 2H^+ \quad (5a)$$

at various pH values. The observed first-order rate constants,

k_5, are listed in Table V along with the calculated concentrations of Hox^- and ox^{2-}.

In Figure 8, $k_5/[Hox]$ is plotted as a function of the $[ox]/[Hox^-]$ ratio. The straight line in this figure suggests the rate law

$$k_5 = k_{5,Hox}[Hox] + k_{5,ox}[ox] \quad (13)$$

The values of $k_{5,Hox}$ and $k_{5,ox}$ were determined to be $7.0 \pm 1.3 \times 10^2$ M^{-1} s^{-1} and $1.29 \pm 0.06 \times 10^4$ M^{-1} s^{-1}, respectively.

It is interesting to compare these rate constants with the values of k_{Hox} and $k_{exptl,ox}$ from eq 3 and 4. For the oxalate-exchange process with $VO(ox)_2^{2-}$, $k_{exptl,Hox}$ was larger than $k_{exptl,ox}$, while $k_{5,ox}$ is much larger than $k_{5,Hox}$ for the formation of $VO(ox)_2^{2-}$. The larger value of $k_{5,ox}$ as compared to the value of $k_{5,Hox}$ can be explained by the assumption that the divalent negative oxalate ion-VO_2^{2+} reaction is primarily a Coulombic process and thus should be faster than the corresponding reaction with the monovalent Hox species. On the other hand, since the $VO(ox)_2^{2-}$ complex has a negative charge, the monovalent Hox^- exchange should be faster than the divalent ox^{2-} exchange with $VO(ox)_2^{2-}$. This is exactly what is observed experimentally.

This ratio of the formation rate constants $k_{5,ox}/k_{5,Hox}$ for reaction 5a corresponds to 18.4 ± 4.2. This value can be compared with the ratio of the theoretically calculated association constants from the Fuoss equation[16] for the reaction between VO^{2+}(aq) and ox^{2-} or Hox^-

$$K_{os(ox)}/K_{os(Hox)} = 23.6$$

The agreement between the calculated and experimental values for these ratios suggests that ligand substitutions on VO^{2+}(aq) are mainly controlled by the electrostatic forces between VO^{2+}(aq) and the various ligands and that the corresponding chelation processes are associative controlled.

Conclusions

It was demonstrated in this paper that ^{13}C NMR spectrometry can be used effectively to determine the rate of ligand-exchange processes for oxovanadium(IV) complexes. These values compare well with the corresponding ^{19}F NMR measurements.

The experiments reported here support the earlier results[4-6] that indicate that ligand-substitution reactions on oxovanadium(IV) complexes are essentially associative. Furthermore, the charge of the entering ligands, $Hmal^-$ and ox^{2-}, is of particular importance in determining the rates for both the ligand-exchange reactions with $VO(ox)_2^{2-}$ and the rate of complex formation for VO^{2+}(aq) to form $VO(ox)_2^{2-}$.

The chelation process starting with $VO(gly)glyF^-$ to form $VO(gly)_2$ is also consistent with the preliminary observations reported earlier,[6] and the results clearly show that the chelation process is associative and is not dissociation (water or anion) controlled.

A similar unidentate ligand complex for the reaction between VO^{2+} and oxalic acid was observed just as in the reactions of glycine[13] and malonic acid[14] with VO^{2+}. The stability constant for the $VOHox^+$ reaction is 10.1 M^{-1}, which is somewhat smaller than the value of 44.7 M^{-1} for the corresponding malonato complex, $VOHmal^-$. The difference between these stability constants can be readily explained from the different pK_2 values for these ligands in that $pK_2(H_2ox) = 1.12$ and $pK_2(H_2mal) = 2.80$.

Registry No. $VO(gly)glyF^-$, 80327-44-2; $VO(ox)_2^{2-}$, 17569-94-7; $VO(gly)_2$, 15283-90-6; F_2, 7782-41-4; $VO(H_2O)_5^{2+}$, 15391-95-4; H_2ox, 144-62-7.

Contribution from the Department of Chemistry, The University of Calgary, Calgary, Alberta, Canada T2N 1N4

Nitrogen-14 Magnetic Resonance Studies of the Effect of Pressure and Temperature on the Rate of Exchange of Acetonitrile Solvent on Iron(II) and Manganese(II) Perchlorates

MARGARET J. SISLEY, YOSHIKO YANO,[1] and THOMAS W. SWADDLE*

Received July 21, 1981

The pressure and temperature dependences of ^{14}N NMR line widths yielded the following activation parameters for the exchange of acetonitrile solvent on iron(II) perchlorate: $\Delta H^* = 41.4$ kJ mol^{-1}, $\Delta S^* = +5.3$ J K^{-1} mol^{-1}, $k^{298} = 6.6 \times 10^5$ s^{-1}, and $\Delta V^*(259\text{-}264\ K) = +3.0$ cm^3 mol^{-1}. For acetonitrile exchange on manganese(II) perchlorate, the parameters were as follows: $\Delta H^* = 29.6$ kJ mol^{-1}, $\Delta S^* = -8.9$ J K^{-1} mol^{-1}, $k^{298} = 1.36 \times 10^7$ s^{-1}, and $\Delta V^*(252\text{-}260\ K) = -7.0$ cm^3 mol^{-1}. Problems concerning the mechanistic significance of these data, and inconsistencies with ΔH^* and ΔS^* values of some earlier reports, are discussed.

We have recently reported the results of a study of the effect of pressure on the rate of exchange of acetonitrile solvent on nickel(II) and cobalt(II),[2] using nitrogen-14 FT NMR line-broadening measurements. That study complemented those of Meyer, Newman, and Merbach[3,4] using proton FT NMR, which is not well suited to this purpose in the case of the cobalt(II) system because, at temperatures high enough to preclude freezing the solvent on application of pressure, the "slow-exchange" approximation of Swift and Connick[5] is no longer applicable; i.e., the ^1H line broadening due to the presence of the paramagnetic ion is not simply related to the solvent-exchange rate from the first coordination sphere.

(1) Visiting Scientist from the Institute of Chemistry, University of Tsukuba, Sakura-Mura, Ibaraki, 300-31 Japan.
(2) Yano, Y.; Fairhurst, M. T.; Swaddle, T. W. *Inorg. Chem.* **1980**, *19*, 3267.
(3) Meyer, F. K.; Newman, K. E.; Merbach, A. E. *Inorg. Chem.* **1979**, *18*, 2142.
(4) Newman, K. E.; Meyer, F. K.; Merbach, A. E. *J. Am. Chem. Soc.* **1979**, *101*, 1470.
(5) Swift, T. J.; Connick, R. E. *J. Chem. Phys.* **1962**, *37*, 307; **1964**, *41*, 2553.

0020-1669/82/1321-1141$01.25/0